Catal Lett (2008) 123:239–245
DOI 10.1007/s10562-008-9413-9

Oxidative Dehydrogenation of C_4 Raffinate-3 to 1,3-Butadiene in a Dual-bed Reaction System Comprising $ZnFe_2O_4$ and $Co_9Fe_3Bi_1Mo_{12}O_{51}$ Catalysts: A Synergistic Effect of $ZnFe_2O_4$ and $Co_9Fe_3Bi_1Mo_{12}O_{51}$ Catalysts

Ji Chul Jung · Howon Lee · Heesoo Kim · Young-Min Chung · Tae Jin Kim · Seong Jun Lee · Seung-Hoon Oh · Yong Seung Kim · In Kyu Song

Received: 13 January 2008 / Accepted: 22 January 2008 /

Abstract Oxidative dehydrogenation of C_4 raffinate-3 to 1,3-butadiene was carried out in a dual-bed reaction system comprising $ZnFe_2O_4$ and $Co_9Fe_3Bi_1Mo_{12}O_{51}$ catalysts in order to investigate a synergistic effect of these two catalysts. Conversion of *n*-butene and yield for 1,3-butiadene obtained in a dual-bed reaction system comprising $ZnFe_2O_4$ (first-bed) and $Co_9Fe_3Bi_1Mo_{12}O_{51}$ (second-bed) were higher than those obtained in a single-bed reaction system using either $ZnFe_2O_4$ or $Co_9Fe_3Bi_1Mo_{12}O_{51}$. 1-Butene-TPD and 2-butene-TPD measurements revealed that $ZnFe_2O_4$ catalyst retained more selective oxygen species for the reaction with 2-butene than for the reaction with 1-butene, while $Co_9Fe_3Bi_1Mo_{12}O_{51}$ catalyst retained more selective oxygen species for the reaction with 1-butene than for the reaction with 2-butene. The synergistic effect of $ZnFe_2O_4$ (first-bed) and $Co_9Fe_3Bi_1Mo_{12}O_{51}$ (second-bed) catalysts in the oxidative dehydrogenation of C_4 raffinate-3 was attributed to the combination of high catalytic activity of $ZnFe_2O_4$ for 2-butene and high catalytic activity of $Co_9Fe_3Bi_1Mo_{12}O_{51}$ for 1-butene.

Keywords Ferrite · Bismuth molybdate · Oxidative dehydrogenation · C_4 raffinate-3 · Synergistic effect

J. C. Jung · H. Lee · H. Kim · I. K. Song (✉)
School of Chemical and Biological Engineering, Institute of Chemical Processes, Seoul National University, Shinlim-dong, Kwanak-ku, Seoul 151-744, South Korea
e-mail: inksong@snu.ac.kr

Y.-M. Chung · T. J. Kim · S. J. Lee · S.-H. Oh · Y. S. Kim
SK Energy Corporation, Yuseong-ku, Daejeon 305-712, South Korea

1 Introduction

1,3-Butadiene is an important raw material for manufacturing a large number of chemical products such as ABS (acrylonitrile-butadiene-styrene), BR (butadiene rubber), and SBR (styrene-butadiene rubber) in the petrochemical industries [1–4]. 1,3-Butadiene currently available in the market is mostly produced through a naphtha cracking process. However, the naphtha cracking process involves many problems in both marketing and energy management, because this process produces not only 1,3-butadiene but also many petrochemical raw materials such as ethylene, propylene, and isobutene [5]. To overcome these problems, oxidative dehydrogenation of *n*-butene to 1,3-butadiene has been extensively studied as a promising process for producing 1,3-butadiene [6–9]. Oxidative dehydrogenation of *n*-butene has many advantages over the conventional naphtha cracking process, because the oxidative dehydrogenation process can be operated as a single unit and is independent of the naphtha cracking unit in producing 1,3-butadiene. Furthermore, no additional major naphtha cracking products (ethylene, propylene, and isobutene) are produced in producing 1,3-butadiene through the oxidative dehydrogenation of n-butene [10, 11].

Three *n*-butene isomers (1-butene, trans-2-butene, and cis-2-butene) or their mixtures have been used as a *n*-butene source in the oxidative dehydrogenation of *n*-butene [12–15]. C_4 raffinate-3 can also be utilized as a *n*-butene source in the oxidative dehydrogenation of *n*-butene for the production of 1,3-butadiene. C_4 raffinate-3 is a residue obtained after separating 1,3-butadiene, isobutene, and 1-butene from C_4 raffinate stream in the naphtha cracking unit. Therefore, C_4 raffinate-3 is mainly composed of 2-butene (trans-2-butene and cis-2-butene), *n*-butane, and unseparated 1-butene. It is expected that the commercial value of C_4 raffinate-3 can be much enhanced if 1,3-butadiene is directly produced using C_4 raffinate-3 as a *n*-butene source.

A large number of metal oxides have been investigated as catalysts in the oxidative dehydrogenation of *n*-butene. These examples include vanadium-containing catalyst [16], ferrite-type catalyst [17–19], manganese oxide molecular sieve catalyst [20], Cu-Mo catalyst [21], and Bi-Mo-based catalyst [22–24]. Among these catalysts, zinc ferrite and multicomponent bismuth molybdate catalysts have been extensively studied as efficient catalysts for this reaction [6, 25, 26]. It was observed in our previous work [27] that the catalytic performance of zinc ferrite ($ZnFe_2O_4$) was dependent on the pH value employed during the co-precipitation step and that $ZnFe_2O_4$ prepared at pH 9 showed the best catalytic performance in the oxidative dehydrogenation of C_4 raffinate-3. It was also revealed that $Co_9Fe_3Bi_1Mo_{12}O_{51}$ served as an efficient multicomponent bismuth molybdate catalyst for the oxidative dehydrogenation of C_4 raffinate-3 [28].

It has been reported that the reactivity of *n*-butene isomers strongly depends on the catalyst system in the oxidative dehydrogenation of *n*-butene [29]. Our preliminary investigations also revealed that the reactivity of *n*-butene isomers over $ZnFe_2O_4$ catalyst decreased in the order of cis-2-butene > trans-2-butene > 1-butene, while that over $Co_9Fe_3Bi_1Mo_{12}O_{51}$ catalyst decreased in the order of 1-butene > cis-2-butene > trans-2-butene. This implies that yield for 1,3-butadiene can be maximized in the oxidative dehydrogenation of C_4 raffinate-3 by combining high catalytic activity of $ZnFe_2O_4$ for 2-butene and high catalytic activity of $Co_9Fe_3Bi_1Mo_{12}O_{51}$ for 1-butene. Therefore, it is expected that a combined catalyst system comprising $ZnFe_2O_4$ and $Co_9Fe_3Bi_1Mo_{12}O_{51}$ would show an enhanced catalytic activity for all *n*-butene isomers in the oxidative dehydrogenation of C_4 raffinate-3, if the catalyst system is properly combined.

In this work, $ZnFe_2O_4$ and $Co_9Fe_3Bi_1Mo_{12}O_{51}$ catalysts were prepared by a co-precipitation method for use in the oxidative dehydrogenation of C_4 raffinate-3 to 1,3-butadiene. A dual-bed reaction system comprising $ZnFe_2O_4$ and $Co_9Fe_3Bi_1Mo_{12}O_{51}$ catalysts was investigated to see any synergistic effect of $ZnFe_2O_4$ and $Co_9Fe_3Bi_1Mo_{12}O_{51}$ catalysts. For comparison, a mechanical mixture of these two catalysts was also applied to the oxidative dehydrogenation of C_4 raffinate-3. 1-Butene-TPD and 2-butene-TPD experiments over $ZnFe_2O_4$ and $Co_9Fe_3Bi_1Mo_{12}O_{51}$ catalysts were carried out to investigate the reactivity of *n*-butene isomers, and thus, to elucidate the synergistic effect of $ZnFe_2O_4$ and $Co_9Fe_3Bi_1Mo_{12}O_{51}$ catalysts.

2 Experimental

2.1 Preparation of $ZnFe_2O_4$ and $Co_9Fe_3Bi_1Mo_{12}O_{51}$ Catalysts

$ZnFe_2O_4$ catalyst was prepared by a co-precipitation method. 1.4 g of zinc chloride ($ZnCl_2$, Sigma-Aldrich) and 5.6 g of iron chloride ($FeCl_3 \cdot 6H_2O$, Sigma-Aldrich) were dissolved in 100 mL of distilled water. The metal precursor solution and an aqueous sodium hydroxide solution (3 N) were then added dropwise into distilled water for co-precipitation under vigorous stirring. During the co-precipitation step, pH of the mixed solution was maintained at 9 using an aqueous sodium hydroxide solution. After the resulting solution was stirred vigorously at room temperature for 12 h, it was aged overnight at room temperature. The precipitate was filtered and washed with deionized water to obtain a solid product. The solid product was dried at 175 °C for 16 h, and finally, it was calcined at 650 °C for 6 h in an air stream to yield the $ZnFe_2O_4$ catalyst.

$Co_9Fe_3Bi_1Mo_{12}O_{51}$ catalyst was also prepared by a co-precipitation method. 1.5 g of bismuth nitrate ($Bi(NO_3)_3$ $5H_2O$, Sigma-Aldrich) was dissolved in 10 mL of distilled water that had been acidified with 3 mL of concentrated nitric acid. The solution was then added to 100 mL of an aqueous solution containing 7.9 g of cobalt nitrate ($Co(NO_3)_2 \cdot 6H_2O$, Sigma-Aldrich) and 3.7 g of ferric nitrate ($Fe(NO_3)_3 \cdot 9H_2O$, Sigma-Aldrich) to obtain a mixed nitrate solution. The mixed nitrate solution was added dropwise into 50 mL of an aqueous solution containing 6.4 g of ammonium molybdate ($(NH_4)_6Mo_7O_{24} \cdot 4H_2O$, Sigma-Aldrich) under vigorous stirring. After stirring the mixed solution at room temperature for 1 h, a solid product was obtained by evaporation. The solid product was dried overnight at 175 °C, and then it was calcined at 475 °C for 5 h in an air stream to yield the $Co_9Fe_3Bi_1Mo_{12}O_{51}$ catalyst.

2.2 Characterization

Formation of $ZnFe_2O_4$ and $Co_9Fe_3Bi_1Mo_{12}O_{51}$ catalysts was confirmed by XRD (MAC Science, M18XHF-SRA) measurements. Atomic ratios of constituent metal components in the prepared catalysts were determined by ICP-AES (Shimadz, ICP-1000IV) analyses. To investigate the selective oxygen species of $ZnFe_2O_4$ and $Co_9Fe_3Bi_1Mo_{12}O_{51}$ catalysts for the reaction with *n*-butene isomers and to elucidate the synergistic effect of these two catalysts in the reaction, 1-butene and 2-butene were used as a probe molecule in the TPD experiments. Each catalyst (0.2 g) was charged into a tubular quartz reactor of the conventional TPD apparatus. The catalyst was pretreated at 200 °C for 1 h under a flow of helium (20 mL/min) to remove any physisorbed organic molecules. 20 mL of *n*-butene (1-butene or 2-butene) was then pulsed into the reactor every minute at room temperature under a flow of helium (5 mL/min), until the adsorption sites of the catalyst were saturated with *n*-butene. 2-Butene was composed of 26.5 wt% trans-2-butene, 72.5 wt% cis-2-butene, and 1.0 wt% residue. The physisorbed *n*-butene was removed by evacuating the catalyst sample at 50 °C for 1 h. The furnace temperature was increased from room temperature to 500 °C at a heating rate of 5 °C/min under a flow of helium (10 mL/min). The desorbed molecules were detected using a GC-MSD (Agilent, MSD-6890N GC).

2.3 Oxidative Dehydrogenation of C_4 Raffinate-3

Oxidative dehydrogenation of C_4 raffinate-3 to 1,3-butadiene was carried out in a continuous flow fixed-bed reactor in the presence of air and steam. For the dual-bed reaction, 0.25 mL of $ZnFe_2O_4$ and 0.25 mL of $Co_9Fe_3Bi_1Mo_{12}O_{51}$ were successively charged into a tubular quartz reactor with a variation of packing sequence, where two catalyst beds were separated by quartz sand. For the single-bed reaction, 0.5 mL of $ZnFe_2O_4$, 0.5 mL of $Co_9Fe_3Bi_1Mo_{12}O_{51}$, or 0.5 mL of a mechanical mixture of $ZnFe_2O_4$ (0.25 mL) and $Co_9Fe_3Bi_1Mo_{12}O_{51}$ (0.25 mL) was charged into a tubular quartz reactor. All the catalysts were pretreated at 470 °C for 1 h with an air stream (16 mL/min). Water was sufficiently vaporized by passing through a pre-heating zone and was continuously fed into the reactor together with *n*-butene and air. Feed composition was fixed at *n*-butene:O_2:steam = 1:0.75:15. C_4 raffinate-3 containing 57.9 wt% *n*-butene (1-butene (7.5 wt%) + trans-2-butene (33.9 wt%) + cis-2-butene (16.5 wt%)) was used as a *n*-butene source, and air was used as an oxygen source (nitrogen in air served as a carrier gas). C_4 raffinate-3 was composed of 57.9 wt% *n*-butene, 41.6 wt% n-butane, 0.3 wt% cyclobutane, 0.1 wt% methyl cyclopropane, and 0.1 wt% residue. The catalytic reaction was carried out at 420 °C. GHSV (gas hourly space velocity) was fixed at 475 h^{-1} on the basis of *n*-butene. Reaction products were periodically sampled and analyzed with gas chromatographs. Conversion of *n*-butene and selectivity for 1,3-butadiene were calculated on the basis of carbon balance as follows. Yield for 1,3-butadiene was calculated by multiplying conversion and selectivity.

$$\text{Conversion of } n\text{-butene} = \frac{\text{moles of } n\text{-butene reacted}}{\text{moles of } n\text{-butene supplied}} \quad (1)$$

$$\text{Selectivity for 1,3-butadiene} = \frac{\text{moles of 1,3-butadiene formed}}{\text{moles of } n\text{-butene reacted}} \quad (2)$$

3 Results and Discussion

3.1 Formation of $ZnFe_2O_4$ and $Co_9Fe_3Bi_1Mo_{12}O_{51}$ Catalysts

Successful formation of $ZnFe_2O_4$ and $Co_9Fe_3Bi_1Mo_{12}O_{51}$ catalysts was confirmed by XRD and ICP-AES measurements. Figure 1 shows the XRD patterns of $ZnFe_2O_4$ and $Co_9Fe_3Bi_1Mo_{12}O_{51}$ catalysts. Each phase was identified by its characteristic diffraction peaks using JCPDS. It was found that $ZnFe_2O_4$ catalyst retained a pure zinc ferrite ($ZnFe_2O_4$) phase and $Co_9Fe_3Bi_1Mo_{12}O_{51}$ catalyst was composed of four major mixed phases of β-$CoMoO_4$, α-$CoMoO_4$, $Fe_2(MoO_4)_3$, and γ-Bi_2MoO_6. These results were well consistent with the previous reports [6, 27]. The atomic ratio of Fe:Zn in the $ZnFe_2O_4$ catalyst was 2.2:1.0, in good agreement with the theoretical value of 2.0:1.0. The atomic ratio of Co:Fe:Bi:Mo in the $Co_9Fe_3Bi_1Mo_{12}O_{51}$ catalyst was measured to be 9.0:3.2:1.0:11.4. This value was also consistent with the theoretical value. The above results indicate that $ZnFe_2O_4$ and $Co_9Fe_3Bi_1Mo_{12}O_{51}$ catalysts were successfully prepared in this work.

3.2 Catalytic Performance in the Oxidative Dehydrogenation of C_4 Raffinate-3

Figure 2 shows the catalytic performance of single- and dual-bed catalysts in the oxidative dehydrogenation of C_4 raffinate-3 to 1,3-butadiene at 420 °C after a 6 h-reaction. The catalytic activity of $ZnFe_2O_4$, $Co_9Fe_3Bi_1Mo_{12}O_{51}$, and

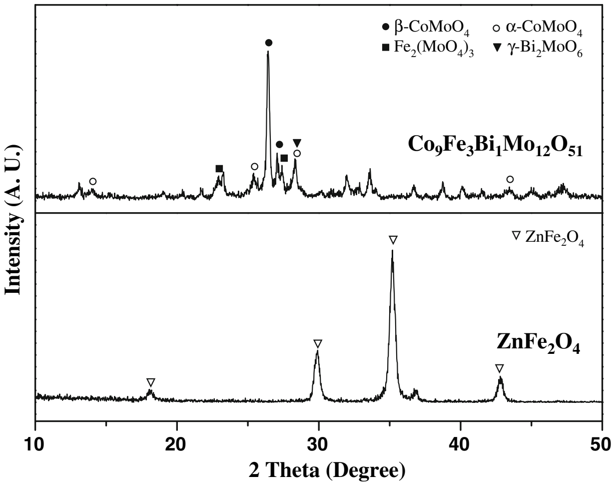

Fig. 1 XRD patterns of $ZnFe_2O_4$ and $Co_9Fe_3Bi_1Mo_{12}O_{51}$ catalysts

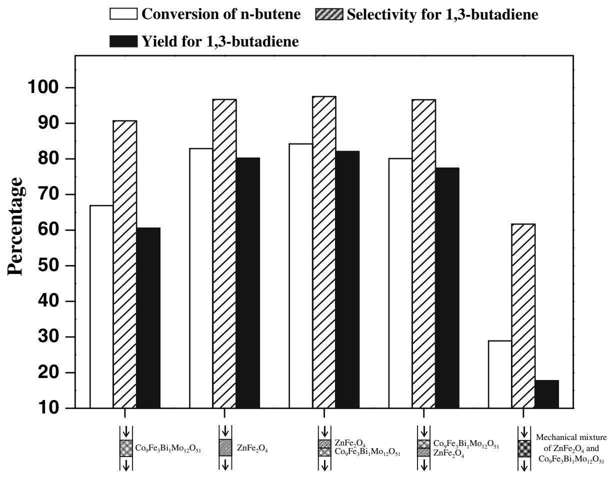

Fig. 2 Catalytic performance of single- and dual-bed catalysts in the oxidative dehydrogenation of C_4 raffinate-3 to 1,3-butadiene at 420 °C after a 6 h-reaction

a mechanical mixture of these two catalysts was tested in a single-bed reaction system. The catalytic activity of dual-bed catalyst system comprising $ZnFe_2O_4$ and $Co_9Fe_3Bi_1Mo_{12}O_{51}$ was examined with a variation of packing sequence of the catalysts. As shown in Fig. 2, $ZnFe_2O_4$ exhibited a better catalytic performance than $Co_9Fe_3Bi_1Mo_{12}O_{51}$ in a single-bed reaction system, in terms of conversion of *n*-butene, selectivity for 1,3-butadiene, and yield for 1,3-butadiene. It is interesting to note that conversion of *n*-butene and yield for 1,3-butiadene obtained with $ZnFe_2O_4$ (first-bed) and $Co_9Fe_3Bi_1Mo_{12}O_{51}$ (second-bed) catalysts in a dual-bed reaction system were higher than those obtained with either $ZnFe_2O_4$ or $Co_9Fe_3Bi_1Mo_{12}O_{51}$ in a single-bed reaction system, indicating a synergistic effect of $ZnFe_2O_4$ and $Co_9Fe_3Bi_1Mo_{12}O_{51}$ catalysts in the dual-bed reaction system. As mentioned earlier, $ZnFe_2O_4$ shows a better catalytic activity for 2-butene than 1-butene, while $Co_9Fe_3Bi_1Mo_{12}O_{51}$ retains a higher catalytic activity for 1-butene than 2-butene in the oxidative dehydrogenation reaction. Therefore, it is believed that the synergistic effect of $ZnFe_2O_4$ (first-bed) and $Co_9Fe_3Bi_1Mo_{12}O_{51}$ (second-bed) catalysts in the dual-bed reaction system was attributed to the combination of high catalytic activity of $ZnFe_2O_4$ and $Co_9Fe_3Bi_1Mo_{12}O_{51}$ for 2-butene and for 1-butene, respectively.

However, conversion of *n*-butene and yield for 1,3-butadiene obtained with $Co_9Fe_3Bi_1Mo_{12}O_{51}$ (first-bed) and $ZnFe_2O_4$ (second-bed) catalysts in a dual-bed reaction system were slightly lower than those obtained with $ZnFe_2O_4$ catalyst in a single-bed reaction system, and furthermore, were lower than those obtained with $ZnFe_2O_4$ (first-bed) and $Co_9Fe_3Bi_1Mo_{12}O_{51}$ (second-bed) catalysts in a dual-bed reactor. C_4 raffinate-3 used as a *n*-butene source in this work contained much more amount of 2-butene (50.4 wt%) than 1-butene (7.5 wt%). Therefore, it is believed that the synergistic effect was only observed in a dual-bed reaction system, where $ZnFe_2O_4$ catalyst showing a high catalytic activity for 2-butene served as a first-bed catalyst. It can be inferred that a synergistic effect is expected in a dual-bed reaction system comprising $Co_9Fe_3Bi_1Mo_{12}O_{51}$ (first-bed) and $ZnFe_2O_4$ (second-bed) catalysts if the content of 1-butene is higher than that of 2-butene in the C_4 raffinate-3 feed.

What is surprising is that the catalytic activity of mechanically mixed catalyst was very low. Although the fundamental reason for this catalytic behavior is not still clear, it can be inferred that each catalyst in the mechanically mixed catalyst impeded the catalysis of the other catalyst in the oxidative dehydrogenation of C_4 raffinate-3. Thus, the simple mechanical mixing of $ZnFe_2O_4$ and $Co_9Fe_3Bi_1Mo_{12}O_{51}$ catalysts was not favorable to cause any synergistic effect of these two catalysts in the oxidative dehydrogenation of C_4 raffinate-3.

In order to clarify the synergistic effect of $ZnFe_2O_4$ (first-bed) and $Co_9Fe_3Bi_1Mo_{12}O_{51}$ (second-bed) catalysts, the reactivity of *n*-butene isomers (1-butene, trans-2-butene, and cis-2-butene) of the C_4 raffinate-3 in the oxidative dehydrogenation reaction was examined. Figure 3 shows the reactivity of *n*-butene isomers of the C_4 raffinate-3 over $ZnFe_2O_4$, $Co_9Fe_3Bi_1Mo_{12}O_{51}$, and $ZnFe_2O_4$ (first-bed)-$Co_9Fe_3Bi_1Mo_{12}O_{51}$ (second-bed) catalysts at 420 °C after a 6 h-reaction. The reactivity of individual *n*-butene isomer was calculated according to the Eq. 3. The reactivity of 2-butene (trans-2-butene and cis-2-butene) was much higher than that of 1-butene over $ZnFe_2O_4$ catalyst, while the reactivity of 1-butene was much higher than that of 2-butene (trans-2-butene and cis-2-butene) over $Co_9Fe_3Bi_1Mo_{12}O_{51}$ catalyst. However, the reactivity of *n*-butene isomers over the dual-bed catalyst system

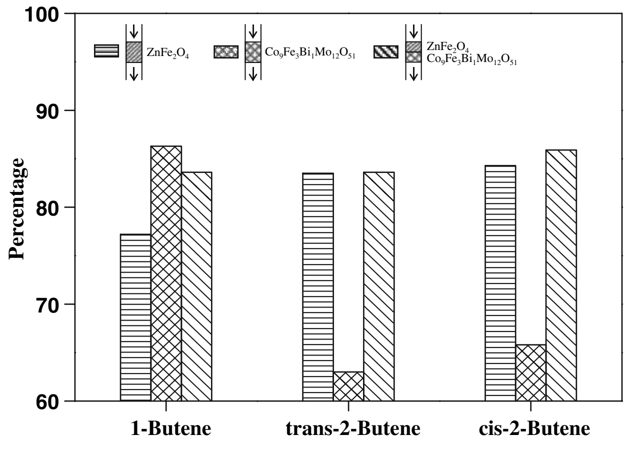

Fig. 3 Reactivity of *n*-butene isomers of the C_4 raffinate-3 over $ZnFe_2O_4$, $Co_9Fe_3Bi_1Mo_{12}O_{51}$, and $ZnFe_2O_4$ (first-bed)-$Co_9Fe_3Bi_1Mo_{12}O_{51}$ (second-bed) catalysts at 420 °C after a 6 h-reaction

($ZnFe_2O_4$ (first-bed) and $Co_9Fe_3Bi_1Mo_{12}O_{51}$ (second-bed)) was consistently high, regardless of the identity of *n*-butene isomers. This result strongly supports the conclusion that the dual-bed reaction system comprising $ZnFe_2O_4$ (first-bed) and $Co_9Fe_3Bi_1Mo_{12}O_{51}$ (second-bed) was much more efficient than the single-bed reaction system in the oxidative dehydrogenation of C_4 raffinate-3.

$$\text{Reactivity of } n\text{-butene isomer} = \frac{\text{moles of } n\text{-butene isomer reacted}}{\text{moles of } n\text{-butene isomer supplied}} \quad (3)$$

3.3 Selective Oxygen Species for the Formation of 1,3-Butadiene

1-Butene-TPD and 2-butene-TPD experiments were conducted in order to investigate the selective oxygen species of $ZnFe_2O_4$ and $Co_9Fe_3Bi_1Mo_{12}O_{51}$ catalysts for the reaction with *n*-butene isomers and to elucidate the different reactivity of *n*-butene isomers over $ZnFe_2O_4$ and $Co_9Fe_3Bi_1Mo_{12}O_{51}$ catalysts. Figure 4 shows the 1-butene-TPD and 2-butene-TPD profiles over $ZnFe_2O_4$ catalyst. In the TPD measurements, the adsorbed *n*-butene (1-butene and 2-butene) was not desorbed in the form of pure component but in the form of 1,3-butadiene and CO_2 by the reaction of *n*-butene with oxygen species in the catalyst. This is in good agreement with the Mars-van Krevelen mechanism, which has been generally accepted for the oxidative dehydrogenation of *n*-butene [30–33]. According to this mechanism, lattice oxygen in the catalyst directly reacts with *n*-butene, and in turn, oxygen in the gas phase makes up the oxygen vacancy in the catalyst. This means that oxygen species in the catalyst directly reacted with *n*-butene to form 1,3-butadiene and CO_2. It can be inferred that the desorbed 1,3-butadiene was attributed to the selective oxygen species in the catalyst involved in the oxidative dehydrogenation of *n*-butene, while the desorbed CO_2 was due to the nonselective oxygen species in the catalyst causing the total oxidation of *n*-butene. This implies that the peak areas of 1,3-butadiene and CO_2 reflect the amount of selective and nonselective oxygen species in the catalyst, respectively. Therefore, major investigations will be focused on the selective oxygen species of the catalyst involved in the formation of 1,3-butadiene.

As shown in Fig. 4, the main peak positions (peak temperatures) of 1,3-butadiene observed in the 1-butene-TPD and 2-butene-TPD profiles were almost identical. However, the peak area of 1,3-butadiene observed in the 2-butene-TPD profile (Fig. 4b) was much larger than that observed in the 1-butene-TPD profile (Fig. 4a). This indicates that $ZnFe_2O_4$ catalyst retained more selective oxygen species for the reaction with 2-butene than for the reaction with 1-butene in the formation of 1,3-butadiene. This result strongly supports that 2-butene was more favorable than 1-butene for the formation of 1,3-butadiene in the oxidative dehydrogenation of *n*-butene over $ZnFe_2O_4$ catalyst.

Figure 5 shows the 1-butene-TPD and 2-butene-TPD profiles over $Co_9Fe_3Bi_1Mo_{12}O_{51}$ catalyst. Like the TPD measurements over $ZnFe_2O_4$ catalyst (Fig. 4), the adsorbed *n*-butene (1-butene and 2-butene) was desorbed in the form of 1,3-butadiene and CO_2 by the reaction of *n*-butene with oxygen species in the catalyst. It is interesting to note that $Co_9Fe_3Bi_1Mo_{12}O_{51}$ catalyst retained two types of selective oxygen species for the reaction with 1-butene to form 1,3-butadiene, while only single type of selective oxygen species existed in the $Co_9Fe_3Bi_1Mo_{12}O_{51}$ catalyst for the reaction with 2-butene to form 1,3-butadiene. Furthermore, the peak area of 1,3-butadiene observed in the 1-butene-TPD profile (Fig. 5a) was much larger than that observed in the 2-butene-TPD profile (Fig. 5b). This indicates that $Co_9Fe_3Bi_1Mo_{12}O_{51}$ catalyst retained more selective oxygen species for the reaction with 1-butene than for the reaction with 2-butene in the formation of 1,3-butadiene, leading to an enhanced reactivity of 1-butene over $Co_9Fe_3Bi_1Mo_{12}O_{51}$ catalyst in the oxidative dehydrogenation of C_4 raffinate-3.

As shown in Figs. 4 and 5, it is noticeable that the main peak positions (peak temperatures) of 1,3-butadiene observed in the 1-butene-TPD and 2-butene-TPD profiles were much lower than those of CO_2 observed in the

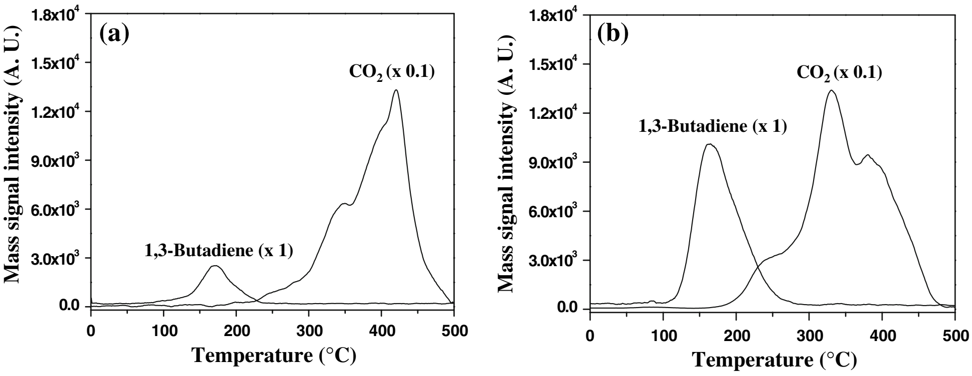

Fig. 4 (**a**) 1-Butene-TPD and (**b**) 2-butene-TPD profiles over $ZnFe_2O_4$ catalyst

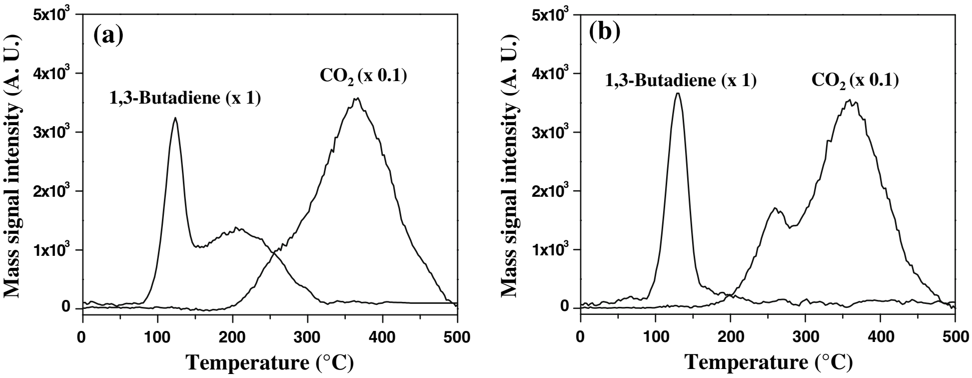

Fig. 5 (**a**) 1-Butene-TPD and (**b**) 2-butene-TPD profiles over $Co_9Fe_3Bi_1Mo_{12}O_{51}$ catalyst

1-butene-TPD and 2-butene-TPD profiles. This means that the selective oxygen species in both catalysts involved in the formation of 1,3-butadiene are more reactive than the nonselective oxygen species in the catalysts causing the total oxidation of *n*-butene. In other words, the selective oxygen species in the catalysts are more mobile than the nonselective oxygen species in the catalysts, although the amount of nonselective oxygen species is much larger than that of selective oxygen species. It is well known that the oxygen mobility is one of the crucial factors determining the catalytic performance in the oxidative dehydrogenation of *n*-butene to 1,3-butadiene [31–33]. What is important in the oxidative dehydrogenation of *n*-butene is not the amount of selective/nonselective oxygen species but the mobility of selective/nonselective oxygen species. Therefore, it is believed that the oxidative dehydrogenation of *n*-butene to 1,3-butadiene mainly occurred by the selective and mobile oxygen species, leading to a high selectivity for 1,3-butadiene in the actual reaction.

It can be concluded that $ZnFe_2O_4$ and $Co_9Fe_3Bi_1Mo_{12}O_{51}$ catalysts retained much amount of selective oxygen species for the reaction with 2-butene and for the reaction with 1-butene, respectively. The synergistic effect of $ZnFe_2O_4$ (first-bed) and $Co_9Fe_3Bi_1Mo_{12}O_{51}$ (second-bed) catalysts in the oxidative dehydrogenation of C_4 raffinate-3 was due to the combination of high catalytic activity of $ZnFe_2O_4$ catalyst for 2-butene and high catalytic activity of $Co_9Fe_3Bi_1Mo_{12}O_{51}$ catalyst for 1-butene under the given C_4 raffinate-3 composition.

4 Conclusions

$ZnFe_2O_4$ and $Co_9Fe_3Bi_1Mo_{12}O_{51}$ catalysts were prepared by a co-precipitation method for use in the oxidative dehydrogenation of C_4 raffinate-3 to 1,3-butadiene. Successful formation of the catalysts was well confirmed by XRD and ICP-AES analyses. Conversion of *n*-butene and yield for 1,3-butadiene obtained in a dual-bed reaction system ($ZnFe_2O_4$ (first-bed) and $Co_9Fe_3Bi_1Mo_{12}O_{51}$ (second-bed)) were higher than those obtained in a single-bed reaction system ($ZnFe_2O_4$ or $Co_9Fe_3Bi_1Mo_{12}O_{51}$) in the oxidative dehydrogenation of C_4 raffinate-3, indicating a synergistic effect of $ZnFe_2O_4$ and $Co_9Fe_3Bi_1Mo_{12}O_{51}$ catalysts. It was found that $ZnFe_2O_4$ and $Co_9Fe_3Bi_1Mo_{12}O_{51}$ catalysts retained much amount of selective oxygen species for the reaction with 2-butene and for the reaction with 1-butene, respectively, in the formation of 1,3-butadiene. Therefore, $ZnFe_2O_4$ showed a high catalytic activity for 2-butene and $Co_9Fe_3Bi_1Mo_{12}O_{51}$ exhibited a high catalytic activity for 1-butene in the oxidative dehydrogenation of C_4 raffinate-3. It is concluded that the synergistic effect of $ZnFe_2O_4$ (first-bed) and $Co_9Fe_3Bi_1Mo_{12}O_{51}$ (second-bed) catalysts in the dual-bed reaction system was attributed to the combination of high catalytic activity of $ZnFe_2O_4$ catalyst for 2-butene and high catalytic activity of $Co_9Fe_3Bi_1Mo_{12}O_{51}$ catalyst for 1-butene under the given C_4 raffinate-3 composition.

Acknowledgments The authors wish to acknowledge support from the Korea Energy Management Corporation (2005-01-0090-3-010).

References

1. Batist PhA, Bouwens JFH, Schuit GCA (1972) J Catal 25:1
2. Grasselli RK (2002) Topics Catal 21:79
3. Linn WJ, Sleight AW (1976) J Catal 41:134
4. Oh SC, Lee HP, Kim HT, Yoo KO (1999) Korean J Chem Eng 16:543
5. Madeira LM, Portela MF (2002) Catal Rev 44:247
6. Moro-oka Y, Ueda W (1994) Adv Catal 40:233
7. Ueda W, Asakawa K, Chen C-L, Moro-oka Y, Ikawa T (1986) J Catal 101:360
8. Wolfs MWJ, Batist PhA (1974) J Catal 32:25
9. He D-H, Ueda W, Moro-oka Y (1992) Catal Lett 12:35
10. Soares APV, Dimitrov LD, Oliveira MCA, Hilaire L, Portela MF, Grasselli RK (2003) Appl Catal A 253:191
11. Kung HH (1994) Adv Catal 40:1
12. van Oeffelen DAG, van Hooff JHC, Schuit GCA (1985) J Catal 95:84
13. Jung JC, Kim H, Choi AS, Chung Y-M, Kim TJ, Lee SJ, Oh S-H, Song IK (2006) J Mol Catal A 259:166
14. Porteal MF (2001) Topics Catal 15:241

15. Egashira M, Matsuo K, Kagawa S, Seiyama T (1979) J Catal 58:409
16. Toledo-Antonio JA, Nava N, Matínez M, Bokhimi X (2002) Appl Catal A 234:137
17. López Nieto JM, Concepción P, Dejoz A, Knözinger H, Melo F, Vázquez MI (2000) J Catal 189:147
18. Kung HH, Kung MC (1985) Adv Catal 33:159
19. Gibson MA, Hightower JW (1976) J Catal 41:431
20. Krishnan VV, Suib SL (1999) J Catal 184:305
21. Tiwari PN, Alkhazov TG, Adzamov KU, Khanmamedova AK (1989) J Catal 120:278
22. Batist PhA, Lippens BC, Schuit GCA (1966) J Catal 5:55
23. Grzybowska B, Haber J, Komorek J (1972) J Catal 25:25
24. Hoefs EV, Monnier JR, Keulks GW (1979) J Catal 57:331
25. Rennard RJ, Kehl WL (1971) J Catal 21:282
26. Ueda W, Chen C-L, Asakawa K, Moro-oka Y, Ikawa T (1986) J Catal 101:369
27. Lee H, Jung JC, Kim H, Chung Y-M, Kim TJ, Lee SJ, Oh S-H, Kim YS, Song IK (2007) Catal Commun, doi: 10.1016/j.catcom.2007.10.023
28. Jung JC, Lee H, Kim H, Chung Y-M, Kim TJ, Lee SJ, Oh S-H, Kim YS, Song IK (2007) Catal Commun, doi: 10.1016/j.catcom.2007.07.031
29. Jung JC, Kim H, Kim YS, Chung Y-M, Kim TJ, Lee SJ, Oh S-H, Song IK (2007) Appl Catal A 317:244
30. Ruckenstein E, Krishnan R, Rai KN (1976) J Catal 45:270
31. Schuit GCA (1974) J Less Comm Metals 36:329
32. Grasselli RK (1997) In: Ertl G, Knözinger H, Weitkamp J (eds) Handbook of heterogeneous catalysis, vol. 5. Wiley, New York, Chapter 4
33. Batist PhA, Der Kinderen AHWM, Leeuwnburgh Y, Metz FAMG, Schuit GCA (1968) J Catal 12:45